FOLIA HISTOCHEMICA ET CYTOBIOLOGICA
Vol. 60, No. 1, 2022
pp. 31–43

ORIGINAL PAPER

VIA MEDICA

EID1 plays a protective role in early-onset pre-eclampsia via promoting proliferation and invasion in trophoblast cells

Ying Li[1, 2], Jiuxiang Feng[1, 3], Yue Bian[1], Wei Cheng[2], Chong Qiao[1, 4, 5, 6, *]

[1]Department of Obstetrics and Gynecology, Shengjing Hospital of China Medical University, Shenyang, Liaoning, China
[2]Department of Obstetrics, Dalian Maternal and Child Health Care Hospital, Dalian, Liaoning, China
[3]Department of Gynecology, Dalian Maternal and Child Health Care Hospital, Dalian, Liaoning, China
[4]Key Laboratory of Maternal-Fetal Medicine of Liaoning Province, Shenyang, Liaoning, China
[5]Key Laboratory of Obstetrics and Gynecology of Higher Education of Liaoning Province, Shenyang, Liaoning, China
[6]Research Center of China Medical University Birth Cohort, Shenyang, Liaoning, China

Abstract

Introduction. Pre-eclampsia is a pregnancy-specific syndrome, which is partly due to abnormal proliferation and invasion of trophoblast cells. EP300 interacting inhibitor of differentiation 1 (EID1) participates in cell proliferation and invasion. This study aims to investigate the roles of EID1 in trophoblast cells and pre-eclampsia.

Material and methods. The expression of EID1 in placental tissues from 60 women with pre-eclampsia and 60 health pregnancies was detected by real-time PCR and immunohistochemical staining. EID1 was overexpressed or silenced by transfection of plasmid or siRNA in HTR-8/SVneo trophoblast cells, and then cell proliferation, cell cycle transition, migration, and invasion were determined by CCK-8 assay, flow cytometry, immunofluorescent staining, immunoblotting, and transwell assays. In addition, the activity of Akt/β-catenin signaling was measured by immunofluorescent staining and Western blot.

Results. EID1 mRNA level was decreased in placental tissues of pre-eclampsia patients, especially early-onset pre-eclampsia, accompanied by more severe clinical manifestation and a higher rate of fetal growth restriction (FGR). Gain- and loss-of-function experiments demonstrated that EID1 promoted proliferation and cell cycle transition, migration, and invasion in HTR-8/SVneo cells and its knockdown played opposite roles, suggesting that EID1 may be required for normal gestation. Akt/β-catenin signaling was activated after EID1 forced expression and deactivated after its silencing.

Conclusions. EID1 promoted proliferation and invasion of cultured trophoblast cells with possible involvement of Akt/β-catenin signaling. These findings may provide novel insights for the diagnosis and treatment of early-onset pre-eclampsia in a clinic. *(Folia Histochemica et Cytobiologica 2022, Vol. 60, No. 1, 31–43)*

Key words: pre-eclampsia, trophoblast cells, EP300 interacting inhibitor of differentiation 1, invasion, pregnancy

***Correspondence address:** Dr. Chong Qiao
Department of Obstetrics and Gynecology,
Shengjing Hospital of China Medical University,
36 Sanhao Street, Heping District, Shenyang 110004, Liaoning, China
phone/fax: +86-24-96615-43416
e-mail: fcchankeren@163.com

Introduction

Pre-eclampsia is a pregnancy-specific syndrome and affects 3–5% of pregnancies [1]. Pre-eclampsia is one of the main causes of maternal, fetal, and neonatal mortality, especially in low-income and middle-income countries [2]. In developing countries,

Folia Histochem Cytobiol. 2022
10.5603/FHC.a2022.0001
ISSN 0239-8508, e-ISSN 1897-5631

www.journals.viamedica.pl/folia_histochemica_cytobiologica

10–15% of direct maternal deaths are associated with pre-eclampsia and eclampsia [3, 4]. Pre-eclampsia is generally diagnosed with hypertension (systolic blood pressure ≥ 140 mm Hg or diastolic blood pressure ≥ 90 mm Hg) and proteinuria (> 300 mg/24 h) [1, 5, 6]. Women with pre-eclampsia generally present with symptoms such as headache, visual disturbances (including blindness), epigastric pain, or nausea and vomiting. Moreover, the cases with severe pre-eclampsia are often accompanied by higher blood pressure (≥ 160/110 mm Hg) or/and multiple organic and systemic damage including hydrothorax, ascites, oligohydramnios, placental abruption, etc. Fetal complications include growth restriction, stillbirth, neonatal death, and prematurity-associated complications from early delivery [1].

Pre-eclampsia is generally divided into two phenotypes, early-onset pre-eclampsia, and late-onset pre-eclampsia, depending on gestational age. Pre-eclampsia diagnosed before 34 gestational weeks is identified as early-onset pre-eclampsia, and that diagnosed at or after 34 gestational weeks as late-onset pre-eclampsia [7]. Late-onset pre-eclampsia accounts for 80–95% of all pre-eclampsia cases, but early-onset pre-eclampsia is associated with more severe clinical manifestations, and poorer maternal and perinatal outcomes [8–10].

The pathogenesis of early and late-onset pre-eclampsia is considered to be different. Valensise *et al.* found that early-onset pre-eclampsia was induced by placental ischemia and hypoxia, while late-onset pre-eclampsia was more associated with maternal microvascular disorder [11]. The central hypothesis of early-onset pre-eclampsia is that the placental ischemia causes poor placentation in 8–18 weeks of pregnancy, then the damaged placenta releases excessive pro-inflammatory and antiangiogenic factors or insufficient amount of placental derived factors into the maternal circulation, and, thus, induces the clinical manifestations of the disease [12]. In pre-eclampsia, the myometrial segment of the spiral artery fails to undergo physiological remodeling during 8–18 weeks of pregnancy, which is thought to explain the defective establishment of uteroplacental circulation followed by uteroplacental ischemia [13]. Human pregnancy is characterized by deep placentation, in which trophoblast cells in the placental bed invade not only the decidua but also one-third the thickness of the myometrium [14]. As invasive trophoblast cells are responsible for the transformation of spiral arteries, some researchers suggested that abnormalities in the trophoblast might result in shallow placentation and inadequate transformation of the spiral arteries, leading to early-onset pre-eclampsia [15, 16]. Therefore, induction/stimulation of proliferation and invasion of trophoblast cells may be helpful for the prevention and treatment of early-onset pre-eclampsia.

EP300 interacting inhibitor of differentiation 1 (EID1) is a transcription repressor, interacting with retinoblastoma protein transcriptional corepressor 1 (RB1) and adenovirus E1A binding protein p300 (EP300) to regulate the expression of myogenic differentiation 1 (MYOD1) [17], and, thus, inhibiting skeletal muscle cell differentiation. EID1 is also named E1A-like inhibitor of differentiation 1, which was demonstrated to inhibit differentiation of osteosarcoma cells [18]. EID1 knockout inhibited the proliferation of mouse neural stem cells [19]. EID1 expression detected by immunohistochemical staining and reverse transcription PCR is increased in invasive intraductal papillary pancreatic mucinous neoplasms (IPMNs), compared with non-invasive IPMNs, suggesting that EID1 may contribute to invasion and metastasis of IPMNs [20]. However, the effects of EID1 on pre-eclampsia or trophoblast cells have not been reported. In our study, we discovered that EID1 was downregulated in placental tissues of pregnancies with pre-eclampsia, especially early-onset pre-eclampsia, compared with that of healthy pregnancies. Moreover, the placental level of EID1 is associated with the severity of early-onset pre-eclampsia. Therefore, gain- and loss-of-function experiments were performed in trophoblast cell cultures to investigate the functions of EID1 in pre-eclampsia.

Material and methods

Clinical specimens. A total of 120 pregnant women participated in this study, including 60 pre-eclampsia cases and 60 healthy controls. These women were recruited in Shengjing Hospital of China Medical University, and informed consent was obtained from everyone. Inclusion criteria included maternal age of 18–40 years old with a singleton pregnancy and a gestational age of more than 20 weeks. The patients with pre-eclampsia diagnosed before 34 gestational weeks were classified as early-onset pre-eclampsia, and those diagnosed at or after 34 gestational weeks as late-onset pre-eclampsia [10]. The healthy pregnancies with equivalent maternal age and gestational age at delivery were considered as early or late control. Both pre-eclampsia cases and healthy volunteers were outpatients from the department of obstetrics and gynecology, Shengjing Hospital of China Medical University (Shenyang), and gestational diabetic patients were excluded. Severe pre-eclampsia was defined with systolic pressure (SP) ≥ 160 mm Hg, diastolic pressure (DP) ≥ 110 mm Hg, proteinuria ≥ 300 mg/24 h, thrombocytopenia, renal insufficiency, impaired liver function, pulmonary edema or cerebral/visual symptoms. Fetal growth restriction (FGR)

Folia Histochem Cytobiol. 2022
10.5603/FHC.a2022.0001
ISSN 0239-8508, e-ISSN 1897-5631

was defined as birth weight ≤ 10th percentile for gestational age. APGAR score was assessed depending on Activity (muscle tone), Pulse (heart rate), Grimace (reflex irritability), Appearance (color), and Respiration (respiratory effort) of a neonate. After delivery, the placental tissues of eclampsia cases or control were collected. Some placental tissues were preserved at –80°C, and others in formaldehyde for pathological examination.

The specimen collection was performed according to the Declaration of Helsinki (1964), and the procedure was approved by the ethical committee of Shengjing Hospital of China Medical University (No. 2017PS230K). Informed consent was obtained from every participant of this study.

Real-time PCR. Total RNA was extracted from placental tissues preserved at –80°C with a Total RNA Extracted Kit (TIANGEN, Beijing, China). Briefly, the tissue of 1 mm^3 was ground in liquid nitrogen and reacted with 1 ml RZ lysis buffer in an Eppendorf tube at room temperature (RT) for 5 min. Then 200 μl of chloroform was added into the tube, which was shocked for 15 s. After standing for 3 min, the reaction product was centrifuged at 10000 g at 4°C for 5 min, and three layers were shown: organic phase, aqueous phase, and the interlayer. The aqueous phase was moved to a new Eppendorf tube and mixed with 0.5 times the volume of ethanol. The mixture was moved into an adsorbing column CR3, centrifuged at 10000 g for 30 s, and the waste liquid was discarded. At this time, RNA and protein were adsorbed in the column. The protein in the column was cleared away by RD reagent and rinsed by RW buffer. After removing the residual liquid, the RNA in the column was dissolved by double-distilled water, and the concentration was determined by NanoDrop Life UV-Vis Spectrophotometer (Thermo Scientific, Waltham, MA, USA). All reagents and instruments used in RNA isolation section were RNase-free. The RNA was reversely transcribed into cDNA with M-MLV reverse transcriptase (TIANGEN). Briefly, 1 μl cDNA, 1 μl oligo(dT) and 1 μl random primer in 9.5 μl water were heated at 70°C for 5 min, and rapidly cooled on ice. Then 2 μl dNTP, 4 μl 5 × buffer, 0.5 μl RNase inhibitor and 1 μl M-MLV were added into the reaction tube, and the mixture was left at 25°C for 10 min, at 42°C for 50 min, and at 80°C for 10 min. The obtained cDNA was used for real-time PCR to detect the mRNA levels of EID1, and the reaction system contained 1 μl cDNA, 1 μl primers (0.5 μl forward primer and 0.5 μl reverse primer), 0.3 μl SYBR GREEN (Solarbio, Beijing, China), 10 μl 2 × Taq PCR MasterMix (TIANGEN) and 7.7 μl water. The PCR procedure was set as follows: 94°C for 5 min 10 s, 60°C for 20 s, 72°C for 30 s, followed with 40 cycles of 72°C for 2 min 30 s, 40°C for 1 min 30 s, melting at 60–90°C every 1°C for 1 s. Finally, the reaction system was incubated at 25°C for several minutes. The data were calculated using $2^{-\Delta\Delta Ct}$ method. GAPDH served as the internal control. The primers were purchased from Genscript (Nanjing, Jiangsu, China). The primers were:

EID1 (NM_014335) forward: 5'-ACTACGACTATCCCGAAGAGG-3';
EID1 reverse: 5'-TGAAACCCGCCATCCAG-3';
GAPDH (NM_002046) forward: 5'-GACCTGACCTGCCGTCTAG-3';
GAPDH reverse: 5'-AGGAGTGGGTGTCGCTGT-3'.

Immunohistochemical staining. The tissues were fixed with 4% paraformaldehyde overnight and washed with tap water. After dehydration, the tissues were embedded in paraffin at 65°C, and paraffin blocks were cut into 5 μm-thick sections. The sections underwent deparaffinization with xylene (15 min twice) and grading concentrations of ethanol (100% for 5 min twice, 95%, 85%, and 75% for 2 min, respectively), placed in boiling antigen retrieval buffer (pH 6.0) in a microwave oven for 5 min, and blocked with 3% H_2O_2 and goat serum for 15 min, respectively. The sections were incubated with rabbit antibodies against EID1 (1:50; Proteintech, Wuhan, Hubei, China) at 4°C overnight. Subsequently, the sections were incubated with goat anti-rabbit IgG-HRP (Thermo Scientific) at 37°C for 60 min and reacted with DAB reagent for several minutes. Finally, hematoxylin was used to stain the nuclei for 3 min, and the sections were mounted with gum. Images were photographed at 400× total magnification.

TUNEL assay. The tissues were made into paraffin sections as the previous description. After deparaffinization, the sections underwent penetration with 0.1% TritonX-100 for 8 min, and were incubated with TUNEL reagent (Roche, Basel, Switzerland) at 37°C for 60 min in the dark. After washing with phosphate-buffered saline (PBS), the sections were counterstained with DAPI for 5 min, and mounted with an anti-fading reagent (Solarbio). The sections were observed with a fluorescence microscope at 400× total magnification.

Construction of plasmids. For overexpression of EID1, the coding sequence was cloned into pcDNA3.1 vector with *HindIII* and *BamHI* sites.

To silence EID1 expression, siRNAs against EID1 coding sequence and negative control (NC) were synthesized. The sense primer and antisense primer were annealed to form the double-stranded siRNA. The sequences of primers were following:
si-NC sense: 5'-UUCUCCGAACGUGUCACGUTT-3';
si-NC antisense: 5'-ACGUGACACGUUCGGAGAATT-3';
si-EID1-1 sense: 5'-CCAACAGCUCGAGGAGGAATT-3';
si-EID1-1 antisense: 5'-UUCCUCCUCGAGCUGUUGGTT-3';
si-EID1-2 sense: 5'-GCGGGUUUCAGAUGCAUUATT-3';
si-EID1-2 antisense: 5'-UAAUGCAUCUGAAACCCGCTT-3'.

The overexpression plasmid and siRNA primers were synthesized by Genscript.

Cell culture. Human HTR-8/SVneo chorionic trophoblast cells were purchased from Zhongqiaoxinzhou (Shanghai, China), and cultured with RPMI-1640 medium supplemented with 10% fetal bovine serum (FBS) at 37°C in 5% CO_2. The cells were adherent cultured and passaged every three days. From the third passage, cells were used for experiments.

Transfection was performed using Lipofectanime™ RNAiMAX Transfection Reagent (Thermo Fisher) in a serum-free medium. Briefly, the cells were cultured in 6-well plates for 24 h for adherence. Then the cells were incubated with a serum-free medium containing 9 μl transfection reagent and 100 pmol siRNA or 2.5 μg plasmid for 4–6 h. Finally, the cells continued to be cultured in a normal medium. 100 pmol siRNA or 2.5 μg plasmid was used for 4×10^5 cells.

Western blot. Total protein was extracted from cultured cells by RIPA lysis buffer, and nuclear protein was extracted with Nuclear Protein Extraction Kit (Solarbio). After concentration determination, an equal amount of protein was used for SDS-PAGE. After electrophoresis, the protein was transferred onto a hydrophobic polyvinylidene fluoride membrane and blocked with skim milk. Then the protein was incubated with following antibodies: rabbit anti-EID1 (1:500; Proteintech), rabbit anti-cyclin D1 (1:500; ABclonal, Wuhan, Hubei, China), rabbit anti-cyclin B1 (1:500; ABclonal), rabbit anti-matrix metalloproteinase (MMP)2 (1:500; Proteintech), rabbit anti-MMP9 (1:1000; Proteintech), rabbit anti-Akt (1:500; ABclonal), rabbit anti-p-Akt (Ser473) (1:500; ABclonal), rabbit anti-glycogen synthase kinase 3 beta (GSK3β) (1:500; ABclonal), rabbit anti-p-GSK3β (Ser9) (1:500; ABclonal), rabbit anti-β-catenin (1:500; ABclonal), mouse anti-GAPDH (1:1000; Proteintech) or rabbit anti-histone H3 (1:5000; GeneTex, Irvine, CA, USA). Subsequently, the protein was incubated with goat anti-rabbit or anti-mouse IgG-HRP (1:3000) at 37°C for 1 h, and reacted with ECL reagent for 5 min. Finally, the signal exposure was performed in the dark.

CCK-8 assay. The HTR-8/SVneo cells were pre-seeded in 96-well plates. After culture for 48 h, the cells were incubated with CCK-8 reagent (KeyGEN, Nanjing, Jiangsu, China) (10 μl per well) for 2 h, and optical density at 450 nm was detected by a microplate reader.

Immunofluorescent staining. The cells were pre-seeded on glass slides. After culture for selected times, the cells were fixed with 4% paraformaldehyde for 15 min, penetrated with 0.1% TritonX-100 for 30 min, and blocked with goat serum for 15 min. The cells were incubated with rabbit antibodies against Ki-67 (1:100; ABclonal) or β-catenin (1:100; ABclonal) at 4°C overnight. After washing with PBS, the cells were incubated with goat anti-rabbit IgG-Cy3 at RT for 30 min in the dark. The nuclei were stained with DAPI. Finally, the slides were mounted with an anti-fading reagent, and observed at 400× total magnification.

Flow cytometry. The cells were pre-cultured in 6-well plates for 48 h. Then the cells were collected and fixed with 70% ethanol at 4°C for 12 h. The cells were washed with PBS twice and stained with propidium iodide (Beyotime, Haimen, Jiangsu, China) (25 μl propidium iodide for 1×10^6 cells) at 37°C for 30 min overnight. Finally, the cells were detected for cell cycle phase distribution with a flow cytometer (ACEA, San Diego, CA, USA).

Transwell assay. Transwell assay was performed to detect the migration and invasion of HTR-8/SVneo cells. The cells were collected and counted. 200 μl suspension containing 5×10^3 cells was added into the transwell upper chamber (Corning, Ithaca, NY, USA) and to the lower chamber, 800 μl of medium containing 10% FBS was added. After culture for 24 h, the cells on the reverse surface were fixed with 4% paraformaldehyde for 25 min and stained with 0.4% crystal violet for 5 min. The numbers of migrating cells were counted with a microscope at 200× magnification.

For invasion detection, the transwell chambers were pre-coated with matrigel, and then the cells were seeded into chambers. Other details were as same as for migration detection.

Statistical analysis. The data in this study were shown as mean ± SD, and analyzed with GraphPad Prism 8.0 (GraphPad Inc, San Diego, CA, USA). The data between two independent groups were analyzed with a student *t*-test, and comparisons among multiple groups were performed with one-way ANOVA with Bonferroni *post-hoc* test. The clinical-pathological characteristics between groups were analyzed with Chi-square test. P value less than 0.05 was considered statistically significant.

Results

EID1 was downregulated in placental tissues of women with pre-eclampsia, especially early-onset pre-eclampsia

60 placenta specimens from pre-eclampsia cases (30 early-onset pre-eclampsia and 30 late-onset pre-eclampsia) and 60 from healthy pregnancies were collected. The maternal age and gestational age between early-onset pre-eclampsia and early-onset control were not statistically different, as well as that between late onset pre-eclampsia and late onset control. The expression of EID1 in these specimens was detected by real-time PCR. As shown in Fig. 1A, the mRNA levels of EID1 were downregulated in placental tissues from pre-eclampsia cases, compared with that in normal pregnant women. Moreover, EID1

Folia Histochem Cytobiol. 2022
10.5603/FHC.a2022.0001
ISSN 0239-8508, e-ISSN 1897-5631

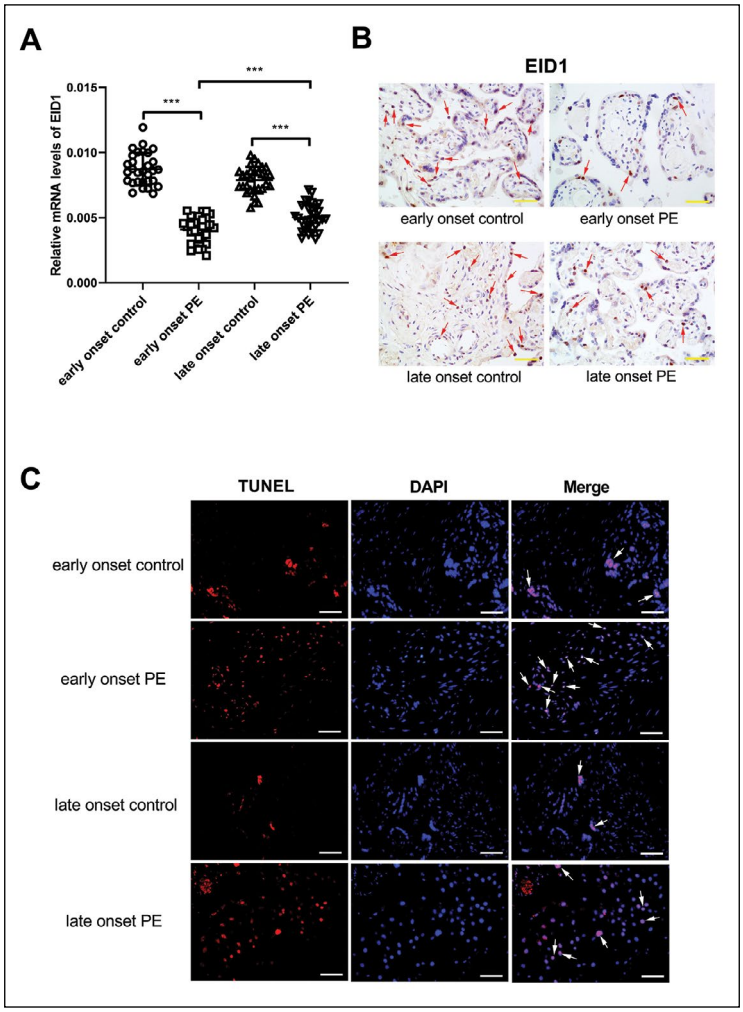

Figure 1. EP300 interacting inhibitor of differentiation 1 (EID1) is downregulated in placental tissues of patients with pre-eclampsia, especially early-onset pre-eclampsia. **A.** Real-time PCR was used to detect the mRNA levels of EID1 in placental tissues of women with early-onset pre-eclampsia, late-onset pre-eclampsia, and normal pregnancy control. **B.** The representative images of immunohistochemical staining for detection of EID1 in placental tissues (arrows indicate EID1-positive cells). **C.** TUNEL assay was performed to examine cell apoptosis in placental tissues, and representative images were shown (arrows indicate TUNEL-positive cells). (Abbreviations: PE — pre-eclampsia. The scale bar represents 50 μm. *p < 0.05.

expression level was lower in placental tissues of cases with early-onset pre-eclampsia, compared with those with late onset pre-eclampsia.

Immunohistochemical staining confirmed the reduction of EID1 protein expression in placental tissues of patients with pre-eclampsia (Fig. 1B). TUNEL assay results showed increased cell apoptosis in placental tissues of women with pre-eclampsia, especially those with early-onset pre-eclampsia, compared with placental tissues from normal pregnancies (Fig. 1C).

In addition, the correlation between EID1 expression and characteristics of the disease was analyzed. Data presented in Table 1 document that EID1 expression was associated with pre-eclampsia severity and FGR. The cases with lower EID1 expression were accompanied by higher SP, a more severe manifestation of pre-eclampsia, and a higher rate of FGR, suggesting that EID1 may be associated with the pathogenesis of early-onset pre-eclampsia.

EID1 promoted proliferation and cell cycle transition of trophoblast cells

Trophoblast cells play crucial roles in pregnancy. To investigate the function of EID1 in trophoblast cells, overexpression plasmid and siRNA of EID1, and their controls were transfected into HTR-8/SVneo cells, respectively. Western blot confirmed the effectiveness of the overexpression and silencing (Fig. 2A). CCK-8 assay results displayed that the viability of HTR-8/SVneo cells was increased after EID1 overexpression and decreased after silencing of EID1 (Fig. 2B). A proliferation marker, Ki-67 was demonstrated to be highly expressed in cells with EID1 overexpression and lower expressed after EID1 knockdown in HTR-8/SVneo cells (Fig. 2C).

Folia Histochem Cytobiol. 2022
10.5603/FHC.a2022.0001
ISSN 0239-8508, e-ISSN 1897-5631

Table 1. Correlation analysis of EID1 expression with maternal and fetal/neonatal characteristics of early-onset pre-eclampsia cases

	EID1 high expression (n = 15)	EID1 low expression (n = 15)	χ^2	p
Age				
≥ 30	9	11	0.6	0.43858
< 30	6	4		
Progestational BMI				
≥ 30	0	2	2.14286	0.14323
< 30	15	13		
Antepartum highest SP [mm Hg]				
≥ 160	9	15	7.5	0.00617**
< 160	6	0		
Antepartum highest DP [mm Hg]				
≥ 110	7	14	1.94444	0.16319
< 110	8	1		
Severity of pre-eclampsia				
Moderate	5	0	6	0.01431*
Severe	10	15		
Neonatal gender				
Boy	7	6	0.13575	0.71255
Girl	8	9		
FGR				
Yes	4	11	6.53333	0.01059*
No	11	4		
Neonatal death				
Yes	2	1	0.37037	0.5428
No	13	14		
Neonate to NICU				
Yes	13	15	2.14286	0.14323
No	2	0		
APGAR score				
≥ 7	8	11	1.29187	0.2557
< 7	7	4		

APGAR — Activity (muscle tone), Pulse (heart rate), Grimace (reflex irritability), Appearance (color) and Respiration; BMI — body mass index; DP — diastolic pressure; EID1 — EP300 interacting inhibitor of differentiation 1; FGR — fetal growth restriction; NICU — neonatal intensive care unit; SP — systolic pressure. *p < 0.05, **p < 0.01.

The flow cytometry results showed that ectopic expression of EID1 accelerated G1/S and G2/M transition and silencing of EID1 led to cell cycle arrest in HTR-8/SVneo cells (Fig. 2D). The two-cell cycle checkpoint proteins, cyclin D1, and cyclin B1, were upregulated by EID1-overexpression and downregulated by EID1 knockdown in HTR-8/SVneo cells (Fig. 2E). Thus, the results presented in this section demonstrated that EID1 promoted the proliferation and cell cycle transition of trophoblast cells.

EID1 enhanced migration and invasion of trophoblast cells

Considering the indispensable roles of trophoblast cell invasion in placentation during pregnancy, the migration and invasion of HTR-8/SVneo cells were determined *in vitro*. As exhibited in transwell results, migration cell numbers were increased after EID1 overexpression and decreased after EID1 knockdown (Fig. 3A). Similar changes were observed in the cell invasion experiment (Fig. 3A).

Folia Histochem Cytobiol. 2022
10.5603/FHC.a2022.0001
ISSN 0239-8508, e-ISSN 1897-5631

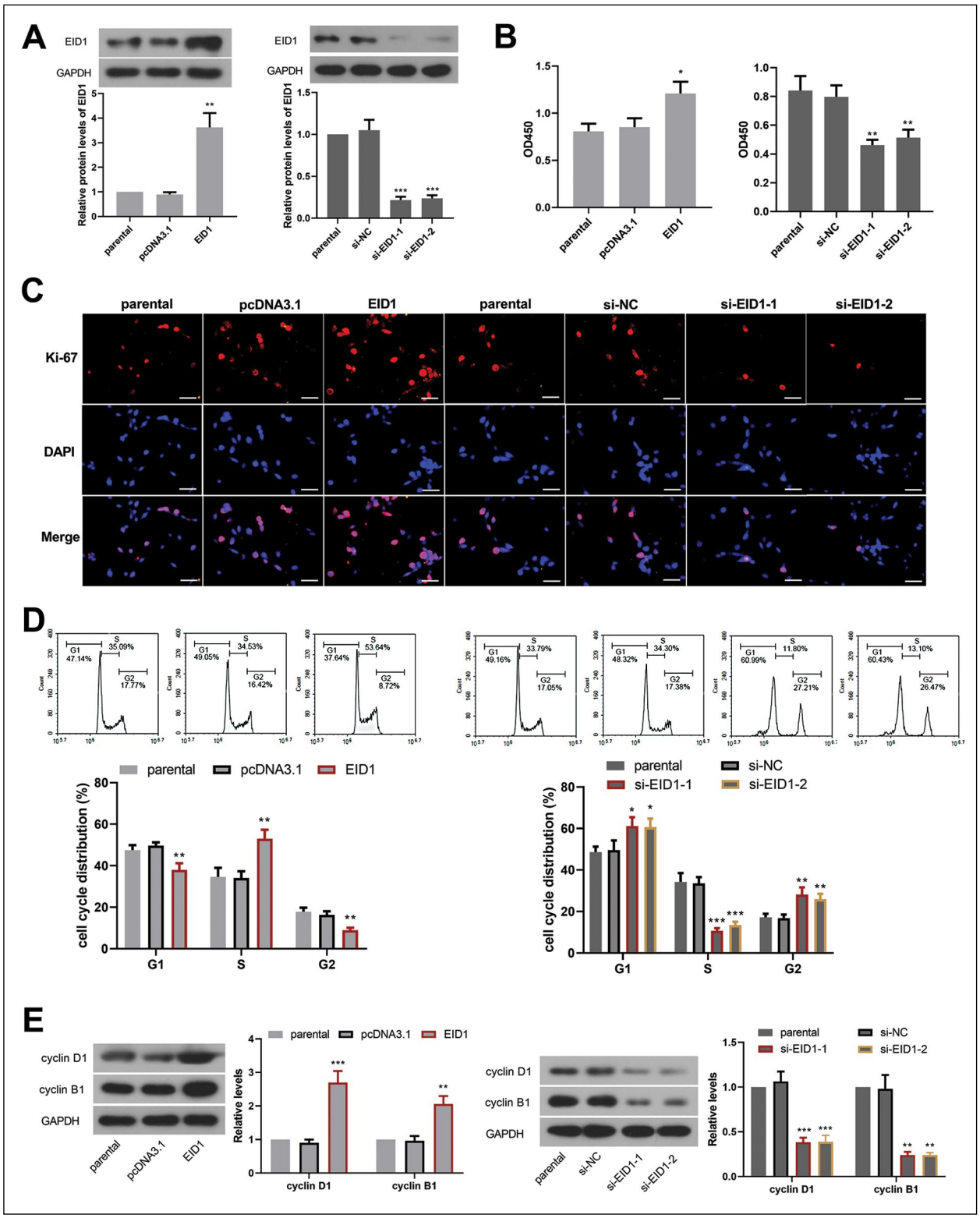

Figure 2. EID1 promoted proliferation and cell cycle transition of trophoblast cells. **A.** Western blot was used to confirm the effectiveness of EID1 overexpression or knockdown in HTR-8/SVneo cells. **B.** Viability of HTR-8/SVeno cells was detected by CCK-8 after culture for 48 h. **C.** The expression of Ki-67 in HTR-8/SVneo cells after EID1 ectopic expression or knockdown was determined by immunofluorescent staining. **D.** Flow cytometry was carried out to detect cell cycle phase distribution of HTR-8/SVneo cells. **E.** The expression of cyclin D1 and cyclin B1 was detected by Western blot. The scale bar represents 50 μm. *p < 0.05, **p < 0.01, ***p < 0.001 compared with pcDNA3.1 or si-NC group.

Folia Histochem Cytobiol. 2022
10.5603/FHC.a2022.0001
ISSN 0239-8508, e-ISSN 1897-5631

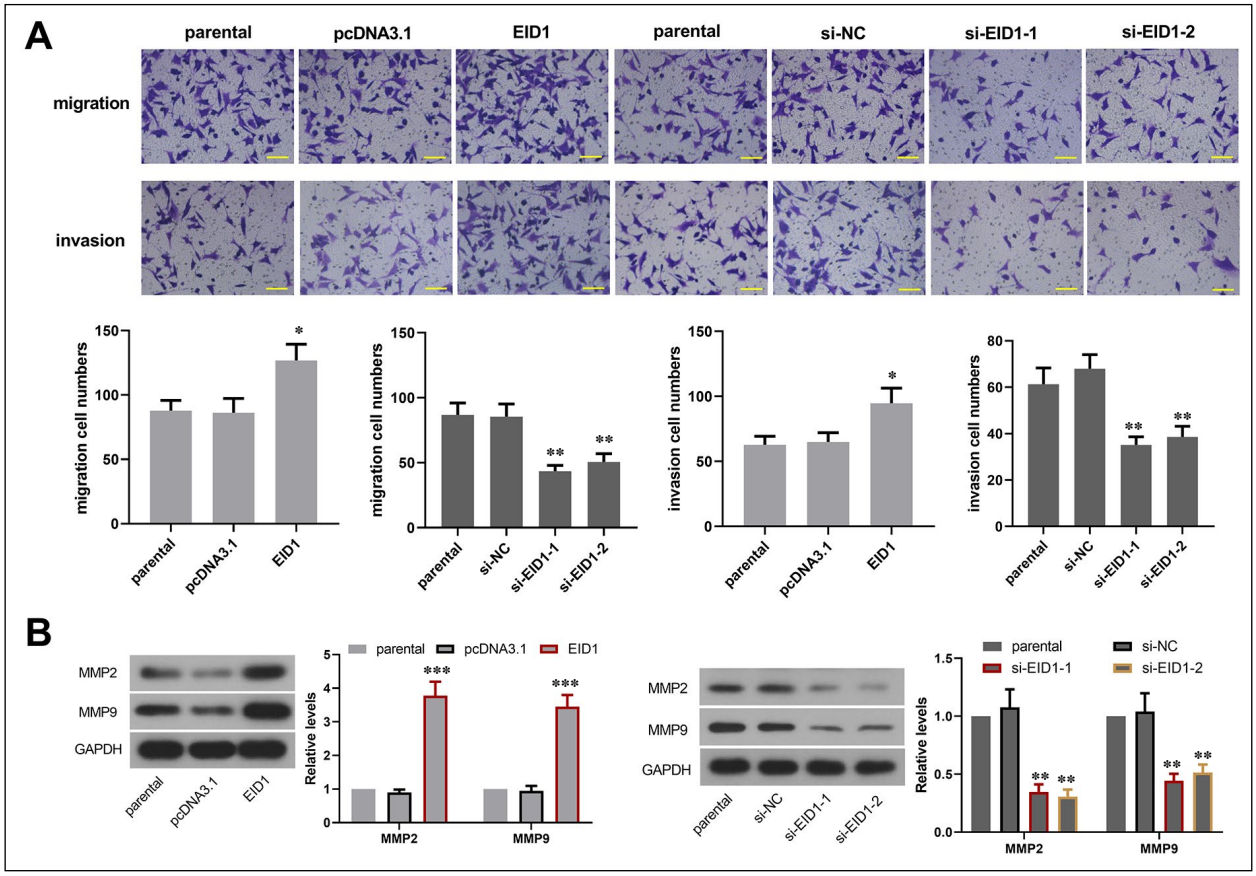

Figure 3. EID1 enhanced migration and invasion of trophoblast cells. **A.** Transwell assay was performed to detect migration and invasion of HTR-8/SVneo cells after overexpression or silencing of EID1. **B.** The expression of MMP2 and MMP9 in HTR-8/SVneo cells was detected by Western blot. The scale bar represents 100 μm. *p < 0.05, **p < 0.01, ***p < 0.001 compared with pcDNA3.1 or si-NC group.

Since degradation of extracellular matrix is essential for invasion, two matrix metalloproteinases, MMP2 and MMP9 were detected. The Western blot results showed that the levels of mature MMP2 and MMP9 were elevated after EID1 overexpression, and declined after EID1 knockdown (Fig. 3B), which was consistent with the results of cell invasion experiments. Thus, the results presented in this section demonstrated that EID1 enhanced migration and invasion of trophoblast cells *in vitro*.

EID1 activated Akt/β-catenin signaling

Because of the notable roles of Akt/β-catenin signaling in cell proliferation and invasion, this pathway was analyzed in the current study. The Western blot results revealed that p-Akt, p-GSK3β, and nuclear β-catenin levels were increased after EID1 overexpression in HTR-8/SVneo cells, suggesting activation of Akt/β-catenin signaling (Fig. 4A and 4C). Conversely, after silencing of EID1, p-Akt, p-GSK3β, and nuclear β-catenin levels were reduced, suggesting deactivation of Akt/β-catenin signaling (Fig. 4B and 4C). Immunofluorescent staining showed that EID1 induced nuclear translocation of β-catenin, which confirmed activation of Akt/β-catenin signaling (Fig. 4D). The results in this section demonstrated that EID1 activated Akt/β-catenin signaling, which may be involved in EID1 function in trophoblast cells.

Discussion

In this study, we found that EID1 was decreased in placental tissues of women with pre-eclampsia, compared with that of healthy pregnancies. Moreover, EID1 expression was particularly low in placental tissues from pregnancies with early-onset pre-eclampsia, accompanied by more severe manifestation of pre-eclampsia, higher rate of FGR, and conspicuous cell apoptosis in placental tissues. The ectopic expression of EID1 promoted proliferation, cell cycle transition, migration, and invasion of HTR-8/SVneo cells and silencing of EID1 played opposite roles. These results suggested that EID1 may be required

Folia Histochem Cytobiol. 2022
10.5603/FHC.a2022.0001
ISSN 0239-8508, e-ISSN 1897-5631

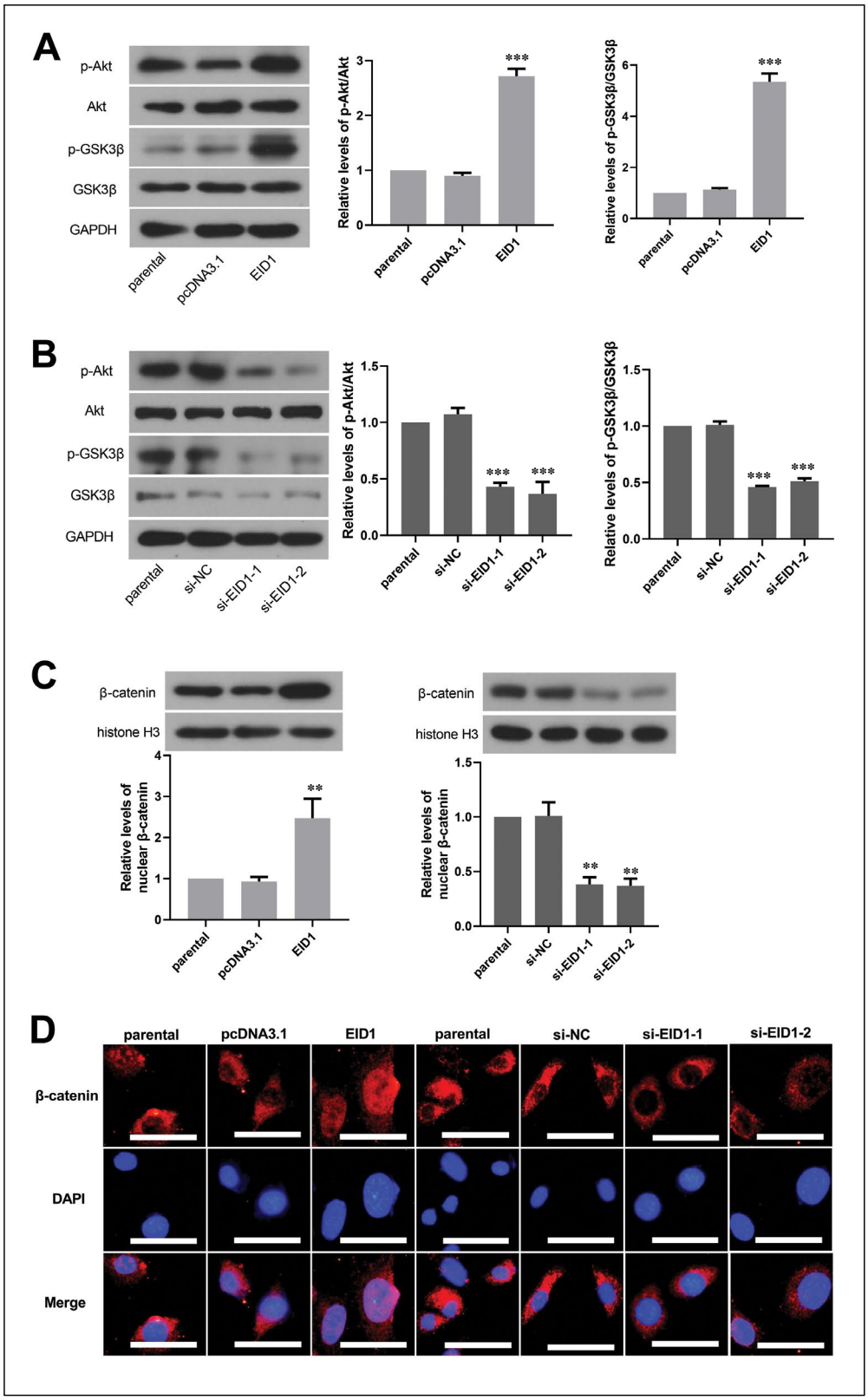

Figure 4. EID1 activated Akt/β-catenin signaling. **A, B.** Western blot was used to detect the levels of Akt, p-Akt (Ser 473), GSK3β, and p-GSK3β (Ser9) in HTR-8/SVneo cells with overexpression or knockdown of EID1. **C.** The nuclear β-catenin levels in HTR-8/SVneo cells were detected. **D.** Immunofluorescent staining was performed to detect the distribution of β-catenin in HTR-8/SVneo cells. The scale bar represents 50 μm. $^{**}p < 0.01$, $^{***}p < 0.001$ compared with pcDNA3.1 or si-NC group.

Folia Histochem Cytobiol. 2022
10.5603/FHC.a2022.0001
ISSN 0239-8508, e-ISSN 1897-5631

for normal gestation. In addition, Akt/β-catenin signaling was activated after EID1 overexpression, and deactivated after EID1 knockdown, suggesting that this signaling may be involved in the mechanisms of EID1 function in trophoblast cells.

Wnt/β-catenin signaling is crucial in cell proliferation and invasion. In the absence of Wnt ligands, cytoplasmic β-catenin binds to the destruction complex composed by Axin, adenomatous polyposis coli (APC), GSK3β, and casein kinase 1α (CK1α). β-catenin exists in a phosphorylated form. The phosphorylated β-catenin is recognized by E3 ubiquitin ligase and then degraded by proteosomes [21, 22]. When Wnt ligand binds to its receptors, the destruction complex is disrupted, and GSK3β is phosphorylated. And then β-catenin is dephosphorylated, accumulates in the cytoplasm, and translocates into nuclei to activate transcription of downstream genes, such as *cylin d1* and *c-myc* [23–25]. It was reported that Wnt1 and β-catenin showed lower expression of mRNA and protein (determined by real-time PCR, Western blot, and immunohistochemical staining) in placentas of pre-eclampsia cases, as well as C-MYC and cyclin D1 [26], whereas the expression of inhibitor of Wnt/β-catenin signaling, Dickkopf-1, was increased [26]. The pre-treatment with LiCl, an activator of Wnt/β-catenin signaling, enhanced the invasion of trophoblast cells under ischemic conditions [27]. In another paper, Chen *et al*. found that a ligand of non-canonical Wnt signaling, Wnt5a, blocked Wnt/β-catenin signaling and reduced migration and invasion of trophoblast cells [28]. In addition to Wnt ligands, β-catenin could be activated by some other molecules. It has been reported that p-Akt could induce the phosphorylation of GSK3β and activation of β-catenin [29]. It was found that Akt inhibitor promoted apoptosis of primary trophoblast cells [30]. These findings suggest that Akt/β-catenin signaling plays a protective role in trophoblast cells invasion. In neural stem cells from mice, EID1 knockout led to the deactivation of Akt/β-catenin signaling [19]. In our study, we demonstrated that the Akt/β-catenin signaling was activated after EID1 overexpression, and deactivated after EID1 knockdown, suggesting that this signaling pathway may be involved in the function of EID1 in trophoblast cells.

EID1 gene was first found in 2000 and named *C15orf3*. It locates in human chromosomes 15q21.1 to q21.2, and encodes a protein molecule of 20.8 kDa ubiquitously expressing in adult tissues [31]. Whereafter, EID1 was identified to bind to RB1 and EP300, and act as a transcription repressor to block the function of transcription factors implicated in differentiation, such as MyoD [18]. EID1 has been demonstrated to inhibit the differentiation of skeletal muscle cells, osteosarcoma cells, and adipocytes [17, 18, 32]. The roles of EID1 have yet not been reported in pre-eclampsia or trophoblast cells.

We demonstrated that EID1 promoted proliferation, migration, and invasion of trophoblast cells, suggesting that EID1 may play a protective role during pre-eclampsia development. Ischemia of the placenta has been considered as the primary reason inducing the clinical manifestations of pre-eclampsia [33], and reduced uteroplacental blood flow was found in women with pre-eclampsia, especially those with early-onset pre-eclampsia [34]. The ischemia is induced by deficiency of the spiral arteries remodeling in the uterus during the early stage of pregnancy, which is identified as the primary inducement of early-onset pre-eclampsia. During a normal pregnancy, uterine blood flow increases to enable perfusion of the intervillous space of the placenta and to support fetal growth. The increased blood flow is achieved by the remodeling of spiral arteries. During this process, trophoblast cells invade the arterial wall, destroy the media and enable the transformation of the spiral arteries from narrow-diameter to large-diameter vessels thereby providing adequate perfusion of the placenta [13, 35]. In pre-eclampsia, the myometrial segment of the spiral artery fails to undergo a physiological transformation in 8–18 weeks of pregnancy [13]. In addition, in the early phase of conceptus implantation, the environment with low oxygen tension stimulates trophoblast cells to proliferate. And in the initial phase of placentation, trophoblast cells differentiate to an invasive phenotype and invade deeper into decidua and myometrium to facilitate the physiological transformation of spiral arteries [36–38]. Deficiency of proliferation and invasion of trophoblast cells may lead to disorders of embryo implantation and placental dysplasia, resulting in an inadequate placental function and restriction of fetal growth.

Our data showed that a higher rate of FGR expression in cases with early-onset pre-eclampsia was accompanied by lower mRNA expression of EID1, which suggested that the decrease of EID1 may be associated with disordered remodeling of spiral arteries in the uterus during the early stage of pregnancy. There have been a lot of papers investigating molecules functioning in trophoblast cells and pre-eclampsia. Annexin A4 (ANXA4), which promoted proliferation and invasion in trophoblast cells, played a protective role in experimental pre-eclampsia rats [39]. α-actinin 4 (ACTIN4) is downregulated in the placenta of pre-eclampsia patients, and its silencing suppressed proliferation and invasion of trophoblast cells. Moreover, ACTIN4-deficient

Folia Histochem Cytobiol. 2022
10.5603/FHC.a2022.0001
ISSN 0239-8508, e-ISSN 1897-5631

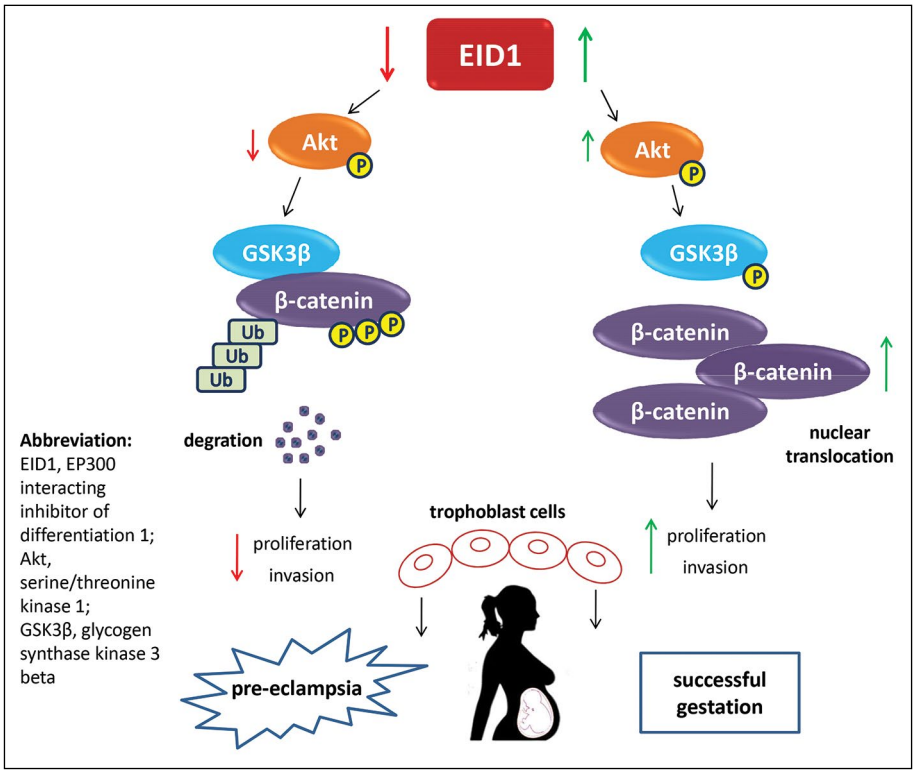

Figure 5. The suggested mechanism of EID1 function. Reduction of EID1 expression deactivated Akt/*β*-catenin signaling, causing the decrease of proliferation and invasion of trophoblast cells, resulting in pre-eclampsia. On the contrary, the high expression of EID1 promoted proliferation and invasion of trophoblast cells by inactivating Akt/*β*-catenin signaling, which may be helpful for successful gestation.

mice exhibited abnormal placentation and pre-eclampsia-like phenotypes [40]. In our study, EID1 promoted proliferation and invasion in trophoblast cells, suggesting that appropriate EID1 expression may be required for a successful pregnancy. However, before attempts to enhance the expression of EID1 aimed at prevention and treatment of early-onset pre-eclampsia in the clinic are made, it is absolutely important to better characterize the cellular and systemic mechanisms of its activity in experimental models of pregnancy. We would induce an experimental pre-eclampsia animal model in the near future to further confirm our hypothesis that EID1 was essential for normal gestation.

Additionally, EID1 is also downregulated in placental tissues of patients with late-onset pre-eclampsia, compared with late-onset control. The pathogenesis of late-onset pre-eclampsia is significantly different from early-onset pre-eclampsia. Although placental hypoxia contributes to late-onset pre-eclampsia, maternal microvascular dysfunction and metabolic disorder play a greater role [7]. EID1 has been reported to inhibit lipid accumulation in mouse preadipocytes [41], suggesting its beneficial effect on lipid metabolism. The effect of EID1 on vascular function is still unclear. Therefore, the roles of EID1 in late-onset pre-eclampsia need to be elucidated by more evidence in the future.

In conclusion, we found that EID1 was decreased in placental tissues of women with early-onset pre-eclampsia, accompanied by more severe clinical manifestation of pre-eclampsia, higher rate of FGR, and more obvious cell apoptosis in placental tissue. The overexpression of EID1 promoted proliferation, migration, and invasion in trophoblast cells, and the silencing of EID1 exhibited opposite effects. Akt/*β*-catenin signaling was activated after EID1 overexpression and deactivated after EID1 knockdown, suggesting that EID1 may function *via* regulating this signaling in trophoblast cells (Fig. 5). These findings may provide novel insights for diagnosis and treatment of early-onset pre-eclampsia in a clinic.

Acknowledgments

This study was funded by grants from the National Key R&D Program of China (2016YFC1000404), the National Natural Science Foundation of China

(81370735), the General Program of National Natural Science Foundation of China (81771610), the Outstanding Scientific Fund of Shengjing Hospital (201706), the Distinguished Professor of Liaoning Province (2017) and the Science and Technology Project of Shenyang (20-205-4-004).

Author's contributions

CQ and YL designed the subject. YL, JF, YB, and WC performed the experiments and analyzed data. YL drafted the manuscript. All authors read and approved the final manuscript.

Availability of data and materials

All of the data and materials are available.

Competing interests

The authors declared that there is no conflict of interest.

References

1. Mol BWJ, Roberts CT, Thangaratinam S, et al. Pre-eclampsia. Lancet. 2016; 387(10022): 999–1011, doi: 10.1016/S0140-6736(15)00070-7, indexed in Pubmed: 26342729.
2. Saleem S, McClure E, Goudar S, et al. A prospective study of maternal, fetal and neonatal deaths in low- and middle-income countries. Bull World Health Organ. 2014; 92(8): 605–612, doi: 10.2471/blt.13.127464, indexed in Pubmed: 25177075.
3. Duley L. Maternal mortality associated with hypertensive disorders of pregnancy in Africa, Asia, Latin America and the Caribbean. Br J Obstet Gynaecol. 1992; 99(7): 547–553, doi: 10.1111/j.1471-0528.1992.tb13818.x, indexed in Pubmed: 1525093.
4. Khan K, Wojdyla D, Say L, et al. WHO analysis of causes of maternal death: a systematic review. The Lancet. 2006; 367(9516): 1066–1074, doi: 10.1016/s0140-6736(06)68397-9, indexed in Pubmed: 16581405.
5. Duley L. The global impact of pre-eclampsia and eclampsia. Semin Perinatol. 2009; 33(3): 130–137, doi: 10.1053/j.semperi.2009.02.010, indexed in Pubmed: 19464502.
6. Brown MA, Magee LA, Kenny LC, et al. International Society for the Study of Hypertension in Pregnancy (ISSHP). Hypertensive Disorders of Pregnancy: ISSHP Classification, Diagnosis, and Management Recommendations for International Practice. Hypertension. 2018; 72(1): 24–43, doi: 10.1161/HYPERTENSIONAHA.117.10803, indexed in Pubmed: 29899139.
7. Burton GJ, Redman CW, Roberts JM, et al. Pre-eclampsia: pathophysiology and clinical implications. BMJ. 2019; 366: l2381, doi: 10.1136/bmj.l2381, indexed in Pubmed: 31307997.
8. Gupta AK, Gebhardt S, Hillermann R, et al. Analysis of plasma elastase levels in early and late onset preeclampsia. Arch Gynecol Obstet. 2006; 273(4): 239–242, doi: 10.1007/s00404-005-0093-z, indexed in Pubmed: 16292578.
9. Lisonkova S, Sabr Y, Mayer C, et al. Maternal morbidity associated with early-onset and late-onset preeclampsia. Obstet Gynecol. 2014; 124(4): 771–781, doi: 10.1097/AOG.0000000000000472, indexed in Pubmed: 25198279.
10. Aneman I, Pienaar D, Suvakov S, et al. Mechanisms of Key Innate Immune Cells in Early- and Late-Onset Preeclampsia. Front Immunol. 2020; 11: 1864, doi: 10.3389/fimmu.2020.01864, indexed in Pubmed: 33013837.
11. Valensise H, Vasapollo B, Gagliardi G, et al. Early and late preeclampsia: two different maternal hemodynamic states in the latent phase of the disease. Hypertension. 2008; 52(5): 873–880, doi: 10.1161/HYPERTENSIONAHA.108.117358, indexed in Pubmed: 18824660.
12. Redman C. The six stages of pre-eclampsia. Pregnancy Hypertens. 2014; 4(3): 246, doi: 10.1016/j.preghy.2014.04.020, indexed in Pubmed: 26104649.
13. Chaiworapongsa T, Chaemsaithong P, Yeo L, et al. Pre-eclampsia part 1: current understanding of its pathophysiology. Nat Rev Nephrol. 2014; 10(8): 466–480, doi: 10.1038/nrneph.2014.102, indexed in Pubmed: 25003615.
14. Brosens I, Pijnenborg R, Vercruysse L, et al. The "Great Obstetrical Syndromes" are associated with disorders of deep placentation. Am J Obstet Gynecol. 2011; 204(3): 193–201, doi: 10.1016/j.ajog.2010.08.009, indexed in Pubmed: 21094932.
15. Zhou Y, Damsky CH, Fisher SJ. Preeclampsia is associated with failure of human cytotrophoblasts to mimic a vascular adhesion phenotype. One cause of defective endovascular invasion in this syndrome? J Clin Invest. 1997; 99(9): 2152––2164, doi: 10.1172/JCI119388, indexed in Pubmed: 9151787.
16. Huppertz B. The Critical Role of Abnormal Trophoblast Development in the Etiology of Preeclampsia. Curr Pharm Biotechnol. 2018; 19(10): 771–780, doi: 10.2174/1389201019666180427110547, indexed in Pubmed: 29701150.
17. MacLellan WR, Xiao G, Abdellatif M, et al. A novel Rb- and p300-binding protein inhibits transactivation by MyoD. Mol Cell Biol. 2000; 20(23): 8903–8915, doi: 10.1128/MCB.20.23.8903-8915.2000, indexed in Pubmed: 11073990.
18. Miyake S, Sellers WR, Safran M, et al. Cells degrade a novel inhibitor of differentiation with E1A-like properties upon exiting the cell cycle. Mol Cell Biol. 2000; 20(23): 8889–8902, doi: 10.1128/MCB.20.23.8889-8902.2000, indexed in Pubmed: 11073989.
19. Fu X, Ding B, Wang C, et al. EID1 plays a crucial role in proliferation of neural stem cell. Biochem Biophys Res Commun. 2019; 512(4): 763–769, doi: 10.1016/j.bbrc.2019.03.138, indexed in Pubmed: 30926163.
20. Kamio Y, Maeda K, Moriya T, et al. Clinicopathological significance of cell cycle regulatory factors and differentiation-related factors in pancreatic neoplasms. Pancreas. 2010; 39(3): 345–352, doi: 10.1097/MPA.0b013e3181bb9204, indexed in Pubmed: 20335778.
21. Rubinfeld B, Albert I, Porfiri E, et al. Binding of GSK3beta to the APC-beta-catenin complex and regulation of complex assembly. Science. 1996; 272(5264): 1023–1026, doi: 10.1126/science.272.5264.1023, indexed in Pubmed: 8638126.
22. Yost C, Torres M, Miller JR, et al. The axis-inducing activity, stability, and subcellular distribution of beta-catenin is regulated in Xenopus embryos by glycogen synthase kinase 3. Genes Dev. 1996; 10(12): 1443–1454, doi: 10.1101/gad.10.12.1443, indexed in Pubmed: 8666229.
23. Pai SG, Carneiro BA, Mota JM, et al. Wnt/beta-catenin pathway: modulating anticancer immune response. J Hematol Oncol. 2017; 10(1): 101, doi: 10.1186/s13045-017-0471-6, indexed in Pubmed: 28476164.
24. Chiurillo MA. Role of the Wnt/β-catenin pathway in gastric cancer: An in-depth literature review. World J Exp Med. 2015; 5(2): 84–102, doi: 10.5493/wjem.v5.i2.84, indexed in Pubmed: 25992323.

25. Nusse R, Clevers H. Wnt/β-Catenin Signaling, Disease, and Emerging Therapeutic Modalities. Cell. 2017; 169(6): 985–999, doi: 10.1016/j.cell.2017.05.016, indexed in Pubmed: 28575679.
26. Wang X, Zhang Z, Zeng X, et al. Wnt/β-catenin signaling pathway in severe preeclampsia. J Mol Histol. 2018; 49(3): 317–327, doi: 10.1007/s10735-018-9770-7, indexed in Pubmed: 29603045.
27. Zhuang B, Luo X, Rao H, et al. Oxidative stress-induced C/EBPβ inhibits β-catenin signaling molecule involving in the pathology of preeclampsia. Placenta. 2015; 36(8): 839–846, doi: 10.1016/j.placenta.2015.06.016, indexed in Pubmed: 26166436.
28. Chen Y, Zhang Yi, Deng Q, et al. Wnt5a inhibited human trophoblast cell line HTR8/SVneo invasion: implications for early placentation and preeclampsia. J Matern Fetal Neonatal Med. 2016; 29(21): 3532–3538, doi: 10.3109/14767058.2016.1138102, indexed in Pubmed: 26865089.
29. Rommel C, Bodine SC, Clarke BA, et al. Mediation of IGF-1-induced skeletal myotube hypertrophy by PI(3)K/Akt/mTOR and PI(3)K/Akt/GSK3 pathways. Nat Cell Biol. 2001; 3(11): 1009–1013, doi: 10.1038/ncb1101-1009, indexed in Pubmed: 11715022.
30. Dash PR, Whitley GS, Ayling LJ, et al. Trophoblast apoptosis is inhibited by hepatocyte growth factor through the Akt and beta-catenin mediated up-regulation of inducible nitric oxide synthase. Cell Signal. 2005; 17(5): 571–580, doi: 10.1016/j.cellsig.2004.09.015, indexed in Pubmed: 15683732.
31. Carim L, Sumoy L, Andreu N, et al. Identification and expression analysis of C15orf3, a novel gene on chromosome 15q21.1-->q21.2. Cytogenet Cell Genet. 2000; 88(3-4): 330–332, doi: 10.1159/000015523, indexed in Pubmed: 10828624.
32. Vargas D, Shimokawa N, Kaneko R, et al. Regulation of human subcutaneous adipocyte differentiation by EID1. J Mol Endocrinol. 2016; 56(2): 113–122, doi: 10.1530/JME-15-0148, indexed in Pubmed: 26643909.
33. Young J, Young J. The AEtiology of Eclampsia and Albuminuria and their Relation to Accidental Haemorrhage: (An Anatomical and Experimental Investigation.). Proc R Soc Med. 1914; 7(Obstet Gynaecol Sect): 307–348, indexed in Pubmed: 19978036.
34. Lunell NO, Nylund LE, Lewander R, et al. Uteroplacental blood flow in pre-eclampsia measurements with indium-113m and a computer-linked gamma camera. Clin Exp Hypertens B. 1982; 1(1): 105–117, doi: 10.3109/10641958209037184, indexed in Pubmed: 7184662.
35. Brosens I, Robertson WB, Dixon HG. The physiological response of the vessels of the placental bed to normal pregnancy. J Pathol Bacteriol. 1967; 93(2): 569–579, doi: 10.1002/path.1700930218, indexed in Pubmed: 6054057.
36. Burton GJ, Hempstock J, Jauniaux E. Nutrition of the human fetus during the first trimester — a review. Placenta. 2001; 22 Suppl A: S70–S77, doi: 10.1053/plac.2001.0639, indexed in Pubmed: 11312634.
37. Jauniaux E, Watson A, Hempstock J, et al. Onset of Maternal Arterial Blood Flow and Placental Oxidative Stress. Am J Pathol. 2000; 157(6): 2111–2122, doi: 10.1016/s0002-9440(10)64849-3, indexed in Pubmed: 11106583.
38. Genbacev O, Joslin R, Damsky CH, et al. Hypoxia alters early gestation human cytotrophoblast differentiation/invasion in vitro and models the placental defects that occur in preeclampsia. J Clin Invest. 1996; 97(2): 540–550, doi: 10.1172/JCI118447, indexed in Pubmed: 8567979.
39. Xu Y, Sui L, Qiu B, et al. ANXA4 promotes trophoblast invasion via the PI3K/Akt/eNOS pathway in preeclampsia. Am J Physiol Cell Physiol. 2019; 316(4): C481–C491, doi: 10.1152/ajpcell.00404.2018, indexed in Pubmed: 30673304.
40. Peng W, Tong C, Li L, et al. Trophoblastic proliferation and invasion regulated by ACTN4 is impaired in early onset preeclampsia. FASEB J. 2019; 33(5): 6327–6338, doi: 10.1096/fj.201802058RR, indexed in Pubmed: 30776251.
41. Sato T, Vargas D, Miyazaki K, et al. EID1 suppresses lipid accumulation by inhibiting the expression of GPDH in 3T3-L1 preadipocytes. J Cell Physiol. 2020; 235(10): 6725–6735, doi: 10.1002/jcp.29567, indexed in Pubmed: 32056205.

Submitted: 28 September, 2021
Accepted after reviews: 27 December, 2021
Available as AoP: 17 January, 2022